POLITECNICO DI TORINO
Repository ISTITUZIONALE

Quantum discord determines the interferometric power of quantum states

Original
Quantum discord determines the interferometric power of quantum states / Girolami, D.; Souza, A. M.; Giovannetti, V.; Tufarelli, T.; Filgueiras, J. G.; Sarthour, R. S.; Soares-Pinto, D. O.; Oliveira, I. S.; Adesso, G.. - In: PHYSICAL REVIEW LETTERS. - ISSN 0031-9007. - 112:21(2014), p. 210401. [10.1103/PhysRevLett.112.210401]

Availability:
This version is available at: 11583/2849565 since: 2020-10-22T16:00:13Z

Publisher:
American Physical Society

Published
DOI:10.1103/PhysRevLett.112.210401

Terms of use:

This article is made available under terms and conditions as specified in the corresponding bibliographic description in the repository

Publisher copyright

(Article begins on next page)

12 October 2024

Quantum Discord Determines the Interferometric Power of Quantum States

Davide Girolami,[1,2,8] Alexandre M. Souza,[3] Vittorio Giovannetti,[4] Tommaso Tufarelli,[5] Jefferson G. Filgueiras,[6] Roberto S. Sarthour,[3] Diogo O. Soares-Pinto,[7] Ivan S. Oliveira,[3] and Gerardo Adesso[1,*]

[1]School of Mathematical Sciences, The University of Nottingham, University Park, Nottingham NG7 2RD, United Kingdom
[2]Department of Electrical and Computer Engineering, National University of Singapore, 4 Engineering Drive 3, 117583 Singapore, Singapore
[3]Centro Brasileiro de Pesquisas Físicas, Rua Dr. Xavier Sigaud 150, Rio de Janeiro, 22290-180 Rio de Janeiro, Brazil
[4]NEST, Scuola Normale Superiore and Istituto Nanoscienze-CNR, Piazza dei Cavalieri 7, I-56126 Pisa, Italy
[5]QOLS, Blackett Laboratory, Imperial College London, London SW7 2BW, United Kingdom
[6]Fakultät Physik, Technische Universität Dortmund, 44221 Dortmund, Germany
[7]Instituto de Física de São Carlos, Universidade de São Paulo, P.O. Box 369, São Carlos, 13560-970 São Paulo, Brazil
[8]Department of Physics, Clarendon Laboratory, University of Oxford, Parks Road, Oxford OX1 3PU, United Kingdom

(Received 11 February 2014; published 27 May 2014)

Quantum metrology exploits quantum mechanical laws to improve the precision in estimating technologically relevant parameters such as phase, frequency, or magnetic fields. Probe states are usually tailored to the particular dynamics whose parameters are being estimated. Here we consider a novel framework where quantum estimation is performed in an interferometric configuration, using bipartite probe states prepared when only the spectrum of the generating Hamiltonian is known. We introduce a figure of merit for the scheme, given by the worst-case precision over all suitable Hamiltonians, and prove that it amounts exactly to a computable measure of discord-type quantum correlations for the input probe. We complement our theoretical results with a metrology experiment, realized in a highly controllable room-temperature nuclear magnetic resonance setup, which provides a proof-of-concept demonstration for the usefulness of discord in sensing applications. Discordant probes are shown to guarantee a nonzero phase sensitivity for all the chosen generating Hamiltonians, while classically correlated probes are unable to accomplish the estimation in a worst-case setting. This work establishes a rigorous and direct operational interpretation for general quantum correlations, shedding light on their potential for quantum technology.

DOI: 10.1103/PhysRevLett.112.210401 PACS numbers: 03.65.Ud, 03.65.Wj, 03.67.Mn, 06.20.-f

All quantitative sciences benefit from the spectacular developments in high-accuracy devices, such as atomic clocks, gravitational wave detectors, and navigation sensors. Quantum metrology studies how to harness quantum mechanics to gain precision in estimating quantities not amenable to direct observation [1–5]. The phase estimation paradigm with measurement schemes based on an interferometric setup [6] encompasses a broad and relevant class of metrology problems, which can be conveniently cast in terms of an input-output scheme [1]. An input probe state ρ_{AB} enters a two-arm channel, in which the reference subsystem B is unaffected while subsystem A undergoes a local unitary evolution, so that the output density matrix can be written as $\rho_{AB}^{\varphi} = (U_A \otimes \mathbb{I}_B)\rho_{AB}(U_A \otimes \mathbb{I}_B)^{\dagger}$, with $U_A = e^{-i\varphi H_A}$, where φ is the parameter we wish to estimate and H_A is the local Hamiltonian generating the unitary dynamics. Information on φ is then recovered through an estimator function $\tilde{\varphi}$ constructed upon possibly joint measurements of suitable dependent observables performed on the output ρ_{AB}^{φ}. For any input state ρ_{AB} and generator H_A, the maximum achievable precision is determined theoretically by the quantum Cramér-Rao bound [3]. Given repetitive interrogations via ν identical copies of ρ_{AB}, this fundamental relation sets a lower limit to the mean square error $\mathrm{Var}_{\rho_{AB}^{\varphi}}(\tilde{\varphi})$ that measures the statistical distance between $\tilde{\varphi}$ and φ, $\mathrm{Var}_{\rho_{AB}^{\varphi}}(\tilde{\varphi}) \geq [\nu F(\rho_{AB}; H_A)]^{-1}$, where F is the quantum Fisher information (QFI) [7], which quantifies how much information about φ is encoded in ρ_{AB}^{φ}. The inequality is asymptotically tight as $\nu \to \infty$, provided the most informative quantum measurement is carried out at the output stage. Using this quantity as a figure of merit for independent and identically distributed trials, and under the assumption of complete prior knowledge of H_A, then "coherence" [8] in the eigenbasis of H_A is the essential resource for the estimation [2]; as maximal coherence in a known basis can be reached by a superposition state of subsystem A only, there is no need for a correlated (e.g., entangled) subsystem B at all in this conventional case.

We show that the introduction of correlations is instead unavoidable when the assumption of full prior knowledge of H_A is dropped. More precisely, we identify, in correlations commonly referred to as "quantum discord" between A and B [9,10], the necessary and sufficient resources rendering physical states able to store phase information in a unitary dynamics, independently of the specific Hamiltonian that generates it. Quantum discord is an indicator of quantumness of correlations in a composite system, usually revealed

 © 2014 American Physical Society

via the state disturbance induced by local measurements [9–12]; recent results suggest that discord might enable quantum advantages in specific computation or communication settings [13–19]. In this Letter a general quantitative equivalence between discord-type correlations and the guaranteed precision in quantum estimation is established theoretically, and is observed experimentally in a liquid-state nuclear magnetic resonance (NMR) proof-of-concept implementation [20,21].

Theory.—An experimenter Alice, assisted by her partner Bob, has to determine, as precisely as possible, an unknown parameter φ introduced by a "black box" device. The black box implements the transformation $U_A = e^{-i\varphi H_A}$ and is controlled by a referee Charlie, see Fig. 1. Initially, only the spectrum of the generator H_A is publicly known, and it is assumed to be nondegenerate. For instance, the experimenters might be asked to monitor a remote (uncooperative) target whose interaction with the probing signals is partially incognito [22]. Alice and Bob prepare ν copies of a bipartite (generally mixed) probe state ρ_{AB} of their choice. Charlie then distributes ν identical copies of the black box, and Alice sends each of her subsystems through one iteration of the box. After the transformations, Charlie reveals the Hamiltonian H_A used in the box, prompting Alice and Bob to perform the best possible joint measurement on the transformed state $(\rho_{AB}^{\varphi})^{\otimes\nu}$ in order to estimate φ [23]. Eventually, the experimenters infer a probability distribution associated to an optimal estimator $\tilde{\varphi}$ for φ saturating the Cramér-Rao bound (for $\nu \gg 1$), so that the corresponding QFI determines exactly the estimation precision. For a given input probe state, a relevant figure of merit for this protocol is then given by the worst-case QFI over all possible black box settings,

$$\mathcal{P}^A(\rho_{AB}) = \frac{1}{4}\min_{H_A} F(\rho_{AB}; H_A), \tag{1}$$

where the minimum is intended over all Hamiltonians with given spectrum (see also [27]), and we inserted a normalization factor $1/4$ for convenience. We shall refer to $\mathcal{P}^A(\rho_{AB})$ as the "interferometric power" (IP) of the input state ρ_{AB}, since it naturally quantifies the guaranteed sensitivity that such a state allows in an interferometric configuration (Fig. 1).

We prove that the quantity in Eq. (1) is a rigorous measure of discord-type quantum correlations of an arbitrary bipartite state ρ_{AB} (see Supplemental Material [27]). If (and only if) the probe state is uncorrelated or only classically correlated, i.e., Alice and Bob prepare a density matrix ρ_{AB} diagonal with respect to a local basis on A [11,13,17], then no precision in the estimation is guaranteed; indeed, in this case there is always a particularly adverse choice for H_A, such that $[\rho_{AB}, H_A \otimes \mathbb{I}_B] = 0$ and no information about φ can be imprinted on the state, resulting in a vanishing IP. Conversely, the degree of discord-type correlations of the state ρ_{AB} not only guarantees but also directly quantifies, via Eq. (1), its usefulness as a resource for estimation of a parameter φ, regardless of the generator H_A of a given spectral class. For generic mixed probes ρ_{AB}, this is true even in the absence of entanglement.

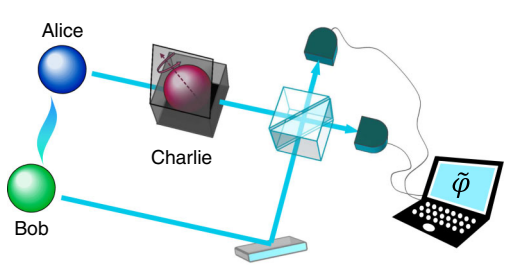

FIG. 1 (color online). Black box quantum estimation.

Remarkably, we can obtain a closed formula for the IP of an arbitrary quantum state of a bipartite system when subsystem A is a qubit. Deferring the proof to [27], this reads

$$\mathcal{P}^A(\rho_{AB}) = \varsigma_{\min}[M] \tag{2}$$

where $\varsigma_{\min}[M]$ is the smallest eigenvalue of the 3×3 matrix M of elements

$$M_{m,n} = \frac{1}{2}\sum_{i,l:\, q_i+q_l\neq 0} \frac{(q_i - q_l)^2}{q_i + q_l} \times \langle\psi_i|\sigma_{mA} \otimes \mathbb{I}_B|\psi_l\rangle\langle\psi_l|\sigma_{nA} \otimes \mathbb{I}_B|\psi_i\rangle$$

with $\{q_i, |\psi_i\rangle\}$ being, respectively, the eigenvalues and eigenvectors of ρ_{AB}, $\rho_{AB} = \sum_i q_i|\psi_i\rangle\langle\psi_i|$. This renders $\mathcal{P}^A(\rho_{AB})$ an operational *and* computable indicator of general nonclassical correlations for practical purposes.

Experiment.—We report an experimental implementation of black box estimation in a room temperature liquid-state NMR setting [20,21]. Here, quantum states are encoded in the spin configurations of magnetic nuclei of a ^{13}C-labeled chloroform ($CHCl_3$) sample diluted in d_6 acetone. The ^{1}H and ^{13}C nuclear spins realize qubits A and B, respectively; the states ρ_{AB} are engineerable as pseudopure states [26,28] by controlling the deviation matrix from a fully thermal ensemble [21]. A highly reliable implementation of unitary phase shifts can be obtained by means of radio frequency (rf) pulses. Referring to [27] for further details of the sample preparation and implementation, we now discuss the plan (Fig. 2) and the results (Fig. 3) of the experiment.

We compare two scenarios, where Alice and Bob prepare input probe states ρ_{AB} either with or without discord. The chosen families of states are, respectively [25,29,30],

$$\rho_{AB}^{Q} = \frac{1}{4}\begin{pmatrix} 1+p^2 & 0 & 0 & 2p \\ 0 & 1-p^2 & 0 & 0 \\ 0 & 0 & 1-p^2 & 0 \\ 2p & 0 & 0 & 1+p^2 \end{pmatrix},$$

$$\rho_{AB}^{C} = \frac{1}{4}\begin{pmatrix} 1 & p^2 & p & p \\ p^2 & 1 & p & p \\ p & p & 1 & p^2 \\ p & p & p^2 & 1 \end{pmatrix}. \tag{3}$$

Both classes of states have the same purity, given by $\mathrm{Tr}[(\rho_{AB}^{Q,C})^2] = (1/4)(1+p^2)^2$, where $0 \le p \le 1$. This

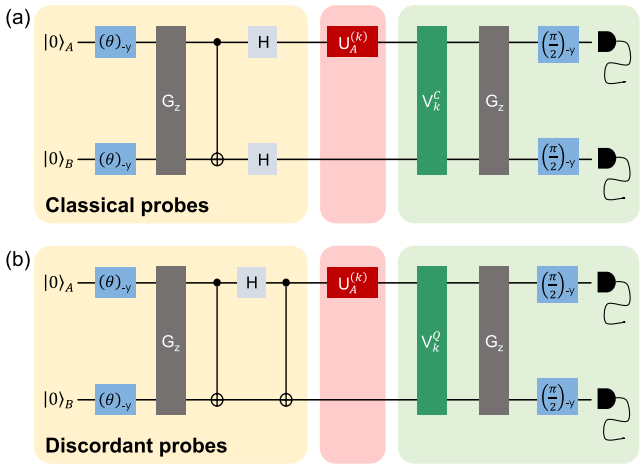

FIG. 2 (color online). Experimental scheme for black box parameter estimation with NMR. The protocol is divided in three steps: probe state preparation (leftmost frame, yellow), black box transformation (middle frame, red), and optimal measurement (rightmost frame, green). Starting from a thermal equilibrium distribution, we initialize the two-qubit system in a pseudopure state of the form $\rho = [(1-\epsilon)/4]\mathbb{I} + \epsilon\rho_{AB}$, with $\epsilon \sim 10^{-5}$ and $\rho_{AB} = |00\rangle\langle 00|_{AB}$. This is done by applying the pulse sequence $(\pi/2)_x \to U_J(1/4J) \to (\pi/2)_y \to U_J(1/4J) \to (\pi/2)_{-x} \to \mathsf{G}_z \to (\pi/4)_y \to U_J(1/2J) \to (\pi/6)_x \to \mathsf{G}_z$, where $(\theta)_\alpha$ is a rotation of each qubit by an angle θ in the direction α, $U_J(\tau)$ is a free evolution under the scalar interaction between the spins for a time τ, and G_z is a pulsed field gradient (which dephases all the spins along the z axis). We then proceed to prepare two types of probe states: the classically correlated ones ρ_{AB}^C (a), and the discordant ones ρ_{AB}^Q (b), defined in Eq. (3). We first apply rf pulses, with a flip angle θ, followed by a pulsed field gradient G_z; this allows us to tune the purity parameter $p = \cos\theta$, by varying θ between 0° and 90° in steps of 2.5°. The subsequent circuits differ for each type of state: for ρ_{AB}^C (a), a CNOT gate followed by Hadamard gates H on both qubits A and B are implemented, while for ρ_{AB}^Q (b), the CNOT is followed by a Hadamard H on qubit A only and by a second CNOT.

allows us to focus on the role of initial correlations for the subsequent estimation, at tunable common degree of mixedness mimicking realistic environmental conditions. While the states ρ_{AB}^C are classically correlated for all values of p, the states ρ_{AB}^Q have discord increasing monotonically with $p > 0$. The probes are prepared by applying a chain of control operations to the initial Gibbs state (Fig. 2). We perform a full tomographical reconstruction of each input state to validate the quality of our state preparation, obtaining a mean fidelity of $(99.7 \pm 0.2)\%$ with the theoretical density matrices of Eq. (3) [27]. In the case of ρ_{AB}^Q, we measure the degree of discord-type correlations in the probes by evaluating the closed formula (2) for the IP on the tomographically reconstructed input density matrices; this is displayed as black crosses in the top panel of Fig. 3 and is found in excellent agreement with the theoretical expectation $\mathcal{P}^A(\rho_{AB}^Q) = p^2$.

Then, for each fixed input probe, and denoting by φ_0 the true value of the unknown parameter φ to be estimated by Alice and Bob (which we set to $\varphi_0 = \pi/4$ in the

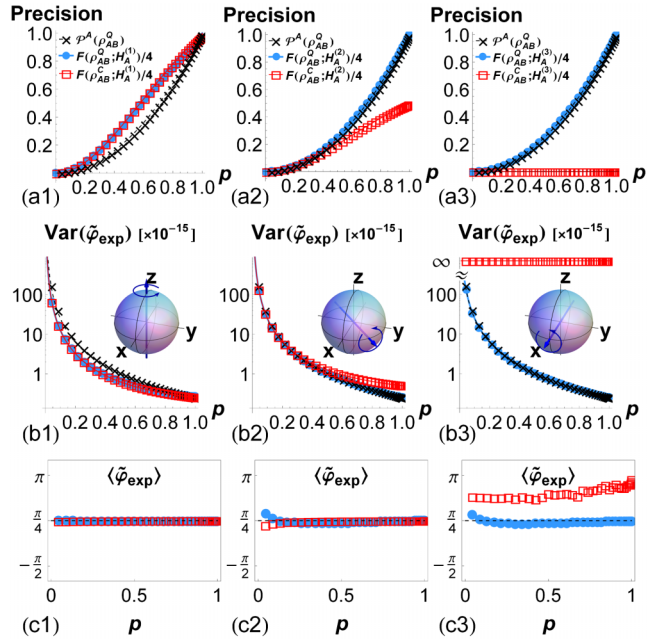

FIG. 3 (color online). Experimental results. Each column corresponds to a different black box setting $H_A^{(k)}$, $k = 1, 2, 3$, generating a φ rotation on qubit A around a Bloch sphere direction $\vec{n}^{(k)}$; the set directions are depicted in the insets of row (b). Empty red squares refer to data from classical probes ρ_{AB}^C, filled blue circles refer to data from discordant probes ρ_{AB}^Q; error bars, due to small pulse imperfections in state preparation and tomography [27], are smaller than the size of the points. The lines refer to theoretical predictions. Both families of states depend on a purity parameter p, experimentally tuned by a flip angle (see Fig. 2). The top row (a) shows the precision achieved by each probe in estimating φ for the different settings: the respective QFIs (divided by 4) as obtained from the output measured data are plotted and compared with the IP $\mathcal{P}^A(\rho_{AB}^Q)$ of the discordant states (black crosses) measured from initial state tomography. The theoretical predictions are: $F_{\rm th}(\rho_{AB}^Q; H_A^{(1)}) = F_{\rm th}(\rho_{AB}^C; H_A^{(1)}) = 8p^2/(1+p^2)$, $F_{\rm th}(\rho_{AB}^Q; H_A^{(2)}) = 4p^2$, $F_{\rm th}(\rho_{AB}^C; H_A^{(2)}) = 4p^2/(1+p^2)$, $F_{\rm th}(\rho_{AB}^Q; H_A^{(3)}) = 4p^2$, $F_{\rm th}(\rho_{AB}^C; H_A^{(3)}) = 0$, and $\mathcal{P}^A(\rho_{AB}^Q) = p^2$. The middle row (b) depicts the measured variances of the optimal estimators $\tilde{\varphi}_{\rm exp}$ over the ensemble of $\nu \approx 10^{15}$ molecules, together with the theoretical predictions corresponding to the saturation of the quantum Cramér-Rao bound. The upper bound limiting the estimation uncertainty for the discordant states is shown as well, given by $4[\nu\mathcal{P}^A(\rho_{AB}^Q)]^{-1}$ as calculated from the input states (crosses). The bottom row (c) depicts the inferred mean value of the optimal estimator $\langle\tilde{\varphi}_{\rm exp}\rangle$ for the various settings. Both classical and quantum probes allow us to obtain a consistently unbiased guess for φ (in the experiment, the true value of φ was set at $\varphi_0 = \pi/4$), apart from the unreliable results of ρ_{AB}^C for $k = 3$, which demonstrates that classical probes cannot return any estimation in the worst-case scenario.

experiments without any loss of generality), we implement three different choices of Charlie's black box transformation $U_A^{(k)} = e^{-i\varphi_0 H_A^{(k)}} \otimes \mathbb{I}_B$. These are given by $H_A^{(1)} = \sigma_{zA}$, $H_A^{(2)} = (\sigma_{xA} + \sigma_{yA})/\sqrt{2}$, and $H_A^{(3)} = \sigma_{xA}$, and are engineered by applying, respectively, the pulse sequences

$U_A^{(1)} = (\pi/2)_x \to (\pi/2)_{-y} \to (\pi/2)_{-x}$, $U_A^{(2)} = (\pi/2)_{x+y}$, and $U_A^{(3)} = (\pi/2)_x$. A theoretical analysis asserts that the chosen settings encompass the best (setting $k = 1$) and worst (setting $k = 3$) case scenarios for both types of probes, while the setting $k = 2$ is an intermediate case [27].

For each input state and black box setting, we carry out the corresponding optimal measurement strategy for the estimation of φ. This is given by projections on the eigenbasis $\{|\lambda_j\rangle\}$ $(j = 1, \ldots, 4)$ of the symmetric logarithmic derivative (SLD) $L_\varphi = \sum_j l_j |\lambda_j\rangle\langle\lambda_j|$, an operator satisfying $\partial_\varphi \rho_{AB}^\varphi = (1/2)(\rho_{AB}^\varphi L_\varphi + L_\varphi \rho_{AB}^\varphi)$ [7]. The QFI is then given by [31]

$$F(\rho_{AB}; H_A) = \mathrm{Tr}[\rho_{AB}^\varphi L_\varphi^2] = 4 \sum_{i<l:\, q_i+q_l\neq 0} \frac{(q_i - q_l)^2}{(q_i + q_l)} |\langle\psi_i|(H_A \otimes \mathbb{I}_B)|\psi_l\rangle|^2,$$

where $\{q_i, |\psi_i\rangle\}$ are the eigenvalues and eigenvectors of ρ_{AB} as before. We implement a readout procedure based on a global rotation into the eigenbasis of the SLD, depicted as $V_k^{C,Q}$ in Fig. 2, followed by a pulsed field gradient G_z to perform an ensemble measurement of the expectation values $d_j = \langle\lambda_j|\rho_{AB}^\varphi|\lambda_j\rangle$ averaged over $\nu \approx 10^{15}$ effectively independent probes [25,27]. These are read from the main diagonal of the output density matrices, circumventing the need for complete state tomography. The measurement basis is selected by a simulated adaptive procedure and the measured ensemble data d_j^{exp} are reported in [27].

To accomplish the estimation, we need a statistical estimator for φ. Denoting by (k, s) an instance of the experiment (with $k = 1, 2, 3$ referring to the black box setting, and $s = C, Q$ referring to the input probes), an optimal estimator for φ which asymptotically saturates the quantum Cramér-Rao bound can be formally constructed as [31,32]

$$\tilde{\varphi}^{(k,s)} = \varphi_0 \mathbb{I} + (L_{\varphi_0}^{(k,s)})/[\sqrt{\nu} F(\rho_{AB}^s; H_A^{(k)})], \tag{4}$$

such that $\langle\tilde{\varphi}^{(k,s)}\rangle = \varphi_0$ and $\mathrm{Var}(\tilde{\varphi}^{(k,s)}) = [\nu F(\rho_{AB}^s; H_A^{(k)})]^{-1}$, because $\langle L_{\varphi_0}^{(k,s)}\rangle = 0$ by definition. However, the estimator in Eq. (4) requires the knowledge of the true value φ_0 of the unknown parameter, which cannot be obtained by iterative procedures in our setup. We then infer directly the ensemble mean and variance of the optimal estimator from the available data, namely, the measured values $d_j^{\mathrm{exp}(k,s)}$ and the knowledge of the input probe states ρ_{AB}^s prepared (and reconstructed) by Alice and Bob, the setting k disclosed by Charlie, and the design eigenvalues l_j of the SLD, which are independent of φ.

First, we infer the expected value of the optimal estimator $\tilde{\varphi}^{(k,s)}$ by means of a statistical least-squares processing. We derive theoretical model expressions for the measured data $d_j^{\mathrm{exp}(k,s)}$ defined by

$$d_j^{\mathrm{th}(k,s)}(\varphi) = \langle\lambda_j^{\varphi_0(k,s)}|(e^{-i\varphi H_A^{(k)}} \otimes \mathbb{I}_B)\rho_{AB}^s(e^{i\varphi H_A^{(k)}} \otimes \mathbb{I}_B)|\lambda_j^{\varphi_0(k,s)}\rangle,$$

and we calculate the value of φ that minimizes the least-squares function $\Upsilon^{(k,s)}(\varphi) = \sum_{j=1}^4 [d_j^{\mathrm{th}(k,s)}(\varphi) - d_j^{\mathrm{exp}(k,s)}]^2$ (equivalent to maximizing the log-likelihood assuming that each d_j is Gaussian distributed over the ensemble). For each setting (k, s), the value of φ that solves the least-squares problem is chosen as the expected value $\langle\tilde{\varphi}_{\mathrm{exp}}^{(k,s)}\rangle$ of our estimator. These values are plotted in row (c) of Fig. 3. One can appreciate the agreement with the true value $\varphi_0 = \pi/4$ of the unknown phase shift for all settings but the pathological one $(C, 3)$. In the latter case, the estimation is completely unreliable because the classical probes commute with the corresponding Hamiltonian generator, thus failing the estimation task.

Next, by expanding the SLD in its eigenbasis (see Table SI in [27]), we obtain the experimental QFIs measured from our data, $F_{\mathrm{exp}}(\rho_{AB}^s; H_A^{(k)}) = \langle(L_{\varphi_0}^{(k,s)})^2\rangle = \sum_j (l_j^{(k,s)})^2 d_j^{\mathrm{exp}(k,s)}$. These are plotted (normalized by a factor $1/4$) for the various settings in row (a) of Fig. 3, together with the lower bound given by the IP of ρ_{AB}^Q. We remark that the QFIs are obtained from the output estimation data, while the IP is measured on the input probe states. In both cases an excellent agreement with theoretical expectations is retrieved for all settings. Notice how in cases $k = 2, 3$ the quantum probes achieve a QFI that saturates the lower bound given by the IP. Notice also that for $k = 3$ the classical states yield strictly zero QFI, as $l_j^{(3,C)} = 0 \forall j$.

Finally, we infer the variance of the optimal estimator over the spin ensemble. This is obtained by replacing $\varphi_0 \mathbb{I}$ with $\langle\tilde{\varphi}_{\mathrm{exp}}^{(k,s)}\rangle \mathbb{I}$ in Eq. (4) and calculating $\mathrm{Var}(\tilde{\varphi}_{\mathrm{exp}}^{(k,s)})$ by expanding it in terms of the design weight values $l_j^{(k,s)}$ and the measured data $d_j^{\mathrm{exp}(k,s)}$; namely, $\mathrm{Var}(\tilde{\varphi}_{\mathrm{exp}}^{(k,s)}) = \{[\sum_j (l_j^{(k,s)})^2 d_j^{\mathrm{exp}(k,s)}] - (\sum_j l_j^{(k,s)} d_j^{\mathrm{exp}(k,s)})^2\}/\{\nu[F_{\mathrm{exp}}(\rho_{AB}^s; H_A^{(k)})]^2\}$. The resulting variances $\mathrm{Var}(\tilde{\varphi}_{\mathrm{exp}}^{(k,s)})$ of our metrology experiment are then plotted in row (b) of Fig. 3. The obtained quantities are in neat agreement with the inverse relation $\mathrm{Var}(\tilde{\varphi}_{\mathrm{exp}}^{(k,s)}) \approx [\nu F_{\mathrm{exp}}(\rho_{AB}^s; H_A^{(k)})]^{-1}$, which allows us to conclude that the implemented estimator with experimentally determined mean $\langle\tilde{\varphi}_{\mathrm{exp}}^{(k,s)}\rangle$ and variance $\mathrm{Var}(\tilde{\varphi}_{\mathrm{exp}}^{(k,s)})$, constructed from our ensemble data, saturates the quantum Cramér-Rao bound: this confirms that an optimal detection strategy was carried out in all settings. Overall, this clearly shows that discord-type quantum correlations, which establish *a priori* the guaranteed precision for any bipartite probe state via the quantifier $\mathcal{P}^A$, are the key resource for black box estimation, demonstrating the central claim of this Letter.

Conclusion.—In summary, we investigated black box parameter estimation as a metrology primitive. We introduced the IP of a bipartite quantum state, which measures its ability to store phase information in a worst-case scenario. This was proven equivalent to a measure of the general quantum correlations of the state. We demonstrated the operational significance of discord-type correlations by implementing a proof-of-concept NMR black box

estimation experiment, where the high controllability on state preparation and gate implementation allowed us to retain the hypothesis of unitary dynamics, and to verify the saturation of the Cramér-Rao bound for optimal estimation. Our results suggest that in highly disordered settings, e.g., NMR systems, and under adverse conditions, quantum correlations even without entanglement can be a promising resource for realizing quantum technology.

We acknowledge discussions with S. Benjamin, T. Bonagamba, T. Bromley, M. Cianciaruso, L. Correa, L. Davidovich, E. deAzevedo, B. Escher, E. Gauger, M. Genoni, M. Guta, S. Huelga, M. S. Kim, M. Lang, B. Lovett, K. Macieszak, K. Modi, J. Morton, M. Paris, M. Piani, R. Serra, and M. Tsang. This work was supported by the Singapore National Research Foundation under NRF Grant No. NRF-NRFF2011-07, the Foundational Questions Institute (FQXI), the University of Nottingham [EPSRC Research Development Fund Grant No. PP-0313/36], the Italian Ministry of University and Research [FIRB-IDEAS Grant No. RBID08B3FM], the Qatar National Research Fund [NPRP 4-426 554-1-084], the Brazilian funding agencies CAPES [Pesquisador Visitante Especial-Grant No. 108/2012], CNPq [PDE Grant No. 236749/2012-9], and FAPERJ, and the Brazilian National Institute of Science and Technology of Quantum Information (INCT/IQ).

*gerardo.adesso@nottingham.ac.uk

[1] V. Giovannetti, S. Lloyd, and L. Maccone, Phys. Rev. Lett. **96**, 010401 (2006).
[2] V. Giovannetti, S. Lloyd, and L. Maccone, Nat. Photonics **5**, 222 (2011).
[3] C. W. Helstrom, *Quantum Detection and Estimation Theory* (Academic Press, New York, 1976).
[4] S. F. Huelga, C. Macchiavello, T. Pellizzari, A. K. Ekert, M. B. Plenio, and J. I. Cirac, Phys. Rev. Lett. **79**, 3865 (1997).
[5] B. M. Escher, R. L. de Matos Filho, and L. Davidovich, Nat. Phys. **7**, 406 (2011).
[6] C. M. Caves, Phys. Rev. D **23**, 1693 (1981).
[7] S. L. Braunstein and C. M. Caves, Phys. Rev. Lett. **72**, 3439 (1994).
[8] T. Baumgratz, M. Cramer, and M. B. Plenio, arXiv:1311.0275 [Phys. Rev. Lett. (to be published)].
[9] H. Ollivier and W. H. Zurek, Phys. Rev. Lett. **88**, 017901 (2001).
[10] L. Henderson and V. Vedral, J. Phys. A. **34**, 6899 (2001).
[11] M. Piani, S. Gharibian, G. Adesso, J. Calsamiglia, P. Horodecki, and A. Winter, Phys. Rev. Lett. **106**, 220403 (2011).
[12] A. Streltsov, H. Kampermann, and D. Bruss, Phys. Rev. Lett. **106**, 160401 (2011).
[13] K. Modi, A. Brodutch, H. Cable, T. Paterek, and V. Vedral, Rev. Mod. Phys. **84**, 1655 (2012).
[14] A. Datta, A. Shaji, and C. M. Caves, Phys. Rev. Lett. **100**, 050502 (2008).
[15] M. Gu, H. M. Chrzanowski, S. M. Assad, T. Symul, K. Modi, T. C. Ralph, V. Vedral, and P. K. Lam, Nat. Phys. **8**, 671 (2012).
[16] B. Dakić *et al.*, Nat. Phys. **8**, 666 (2012).
[17] D. Girolami, T. Tufarelli, and G. Adesso, Phys. Rev. Lett. **110**, 240402 (2013).
[18] M. de Almeida, M. Gu, A. Fedrizzi, M. A. Broome, T. C. Ralph, and A. White, Phys. Rev. A **89**, 042323 (2014).
[19] S. Pirandola, arXiv:1309.2446.
[20] R. R. Ernst, G. Bodenhausen, and A. Wokaum, *Principles of Nuclear Magnetic Resonance in One and Two Dimensions* (Oxford University Press, New York, 1987).
[21] I. S. Oliveira, T. J. Bonagamba, R. S. Sarthour, J. C. C. Freitas, and E. R. deAzevedo, *NMR Quantum Information Processing* (Elsevier, New York, 2007).
[22] S. Lloyd, Science **321**, 1463 (2008).
[23] This setting is very natural for implementations such as NMR, where measurements on an ensemble of ν probes are taken collectively, rather than iteratively [24–26].
[24] J. A. Jones, S. D. Karlen, J. Fitzsimons, A. Ardavan, S. C. Benjamin, G. A. D. Briggs, and J. J. L. Morton, Science **324**, 1166 (2009).
[25] M. Schaffry, E. M. Gauger, J. J. L. Morton, J. Fitzsimons, S. C. Benjamin, and B. W. Lovett, Phys. Rev. A **82**, 042114 (2010).
[26] D. G. Cory, A. F. Fahmy, and T. F. Havel, Proc. Natl. Acad. Sci. U.S.A. **94**, 1634 (1997).
[27] See Supplemental Material at http://link.aps.org/supplemental/10.1103/PhysRevLett.112.210401 for technical proofs and additional experimental details. The Supplemental Material document contains additional Refs. [33–45].
[28] N. A. Gershenfeld and I. L. Chuang, Science **275**, 350 (1997).
[29] S. Simmons, J. A. Jones, S. D. Karlen, A. Ardavan, and J. J. L. Morton, Phys. Rev. A **82**, 022330 (2010).
[30] K. Modi, H. Cable, M. Williamson, and V. Vedral, Phys. Rev. X **1**, 021022 (2011).
[31] M. G. A. Paris, Int. J. Quantum. Inform. **07**, 125 (2009).
[32] Here and in the following, the averages are intended to be calculated on the transformed states $\rho_{AB}^{\varphi s}$ after the black box.
[33] S. Luo, Phys. Rev. Lett. **91**, 180403 (2003).
[34] E. P. Wigner and M. M. Yanase, Proc. Natl. Acad. Sci. U.S.A. **49**, 910 (1963).
[35] B. Aaronson, R. Lo Franco, and G. Adesso, Phys. Rev. A **88**, 012120 (2013).
[36] A. Abragam, *The Principles of Nuclear Magnetism* (Oxford University Press, New York, 1978).
[37] L. M. K. Vandersypen and I. L. Chuang, Rev. Mod. Phys. **76**, 1037 (2005).
[38] N. A. Gershenfeld and I. L. Chuang, Science **275**, 350 (1997).
[39] S. L. Braunstein, C. M. Caves, R. Jozsa, N. Linden, S. Popescu, and R. Schack, Phys. Rev. Lett. **83**, 1054 (1999).
[40] N. Linden and S. Popescu, Phys. Rev. Lett. **87**, 047901 (2001).
[41] J. A. Jones, Prog. Nucl. Magn. Reson. Spectrosc. **59**, 91 (2011).
[42] M. A. Nielsen and I. L. Chuang, *Quantum Computation and Quantum Information* (Cambridge University Press, Cambridge, England, 2000).
[43] I. L. Chuang, N. Gershenfeld, M. Kubinec, and D. Leung, Proc. R. Soc. A **454** 447 (1998).
[44] G. M. Leskowitz and L. J. Mueller, Phys. Rev. A **69**, 052302 (2004).
[45] X. Wang, C.-S. Yu, and X.-X. Yi, Phys. Lett. A **373**, 58 (2008).